

Sodium-doped dimer rows on Si(001)

M. J. Haye, P. M. L. O. Scholte, A. F. Bakker, S. W. de Leeuw, and F. Tuinstra

Department of Applied Physics, Delft University of Technology, Lorentzweg 1, 2628 CJ Delft, The Netherlands

G. Brocks

Philips Research Laboratories, Professor Holstlaan 4, 5656 AA Eindhoven, The Netherlands

(Received 26 February 1997)

The stability and electronic structure of a nanowire are studied by first-principles calculations. The wire consists of a single depassivated silicon dimer row on the hydrogen passivated Si(001) 2×1 surface. We predict that sodium atoms evaporated onto this surface stick preferentially at the depassivated row and partially fill the empty one-dimensional states of this row. This leads to a thin metallic wire of atomic size dimensions. At room temperature the sodium atoms are mobile along the depassivated row; they become immobile at temperatures below ~ 120 K. [S0163-1829(97)50328-6]

Nanowires have attracted considerable attention as such small one-dimensional (1D) structures are expected to exhibit intriguing physical properties such as a quantized conductance or a transition to a Tomonaga-Luttinger liquid at low temperatures.¹ In recent years rapid progress has been made in manipulating atoms with the scanning tunneling microscope (STM), which makes it possible to build 1D structures atom by atom.² On metallic substrates the 1D electronic states of such structures are usually strongly mixed with the bulk metal states. In order to study unperturbed 1D effects, one would therefore prefer to use semiconducting (or insulating) substrates. Recent examples of stable 1D structures on semiconductor surfaces constructed using STM techniques, are atomic scale grooves on the Si(111) surface³ and depassivated single dimer rows on the 2×1 monohydride Si(001) surface.⁴ Both these structures are semiconducting, however, and a necessary condition for the occurrence of the low-temperature effects mentioned above is that the structures have 1D metallic character at higher (e.g., room) temperature. The challenge therefore is to construct an atomic scale metallic wire on a semiconducting substrate. There are a number of possible approaches. One could, for instance, modify a specific surface in order to create a wire which is intrinsically metallic. An example of this was explored in recent theoretical work where the possibility of a stable “dangling bond wire” on hydrogen passivated Si(111) was discussed.⁵ Another possibility is to use semiconducting 1D structures as templates for metal atoms evaporated onto the surface, the experimental feasibility of which has recently been demonstrated quite convincingly by Shen *et al.*⁶ The microscopic limit of a single row of metal atoms (which interact strongly with the substrate) will not necessarily result in a conducting wire. For example, first-principles calculations by Brocks *et al.* show that lines of aluminum atoms on Si(001) are semiconducting.⁷ A third approach is to dope semiconducting 1D structures. Some of these structures have states inside the bulk band gap, which have a pure 1D character. Transferring electrons (holes) from dopant atoms to empty (filled) 1D states would result in conducting wires.

In this paper we propose a specific realization of this last approach and study it by means of first-principles calculations.

We start from a single depassivated dimer (DD) row on the 2×1 hydrogen passivated (i.e., monohydride) Si(001) surface. The 1D bands that result from the dangling bonds on the depassivated dimers of that row consist of filled π and empty π^* bands, both partly inside the bulk Si band gap. We propose to use sodium atoms evaporated onto the surface in order to inject electrons into the empty band. Previous calculations for high coverages of Na on the clean Si(001) surface have shown that the surface band structure is virtually unchanged, apart from a partial filling of the empty surface states.⁸ One could expect the DD row to behave similarly, provided that the Na dopant atoms can be localized near the DD row. We will study to what extent the DD row acts as a preferential adsorption site for Na adatoms. The resulting electronic structure will be discussed and we present evidence for the metallic character of this row.

In the calculations we use a Car-Parrinello-like technique for the simultaneous optimization of the electronic and ionic degrees of freedom.⁹ The Si(001) surface is modeled in a supercell by a slab consisting of six layers of Si, saturated at the bottom by hydrogen atoms. The repeated slabs are separated by a vacuum region of 10.5 \AA . The positions of the atoms in the bottom two layers of the slab plus the H atoms, are kept fixed. The Si and Na ion cores are modeled by separable¹⁰ norm conserving pseudopotentials^{11,12} with s and p nonlocal components; for H we use a local potential. The local-density approximation for the exchange and correlation is used,¹³ with a nonlinear core correction applied to the Na ions.¹⁴ A plane-wave kinetic energy cutoff of 12 Ry is used, with the exception of the sodium adsorption on the clean Si(001) surface, where we use 8 Ry. The \mathbf{k} -point sampling is equivalent to eight points in the $p(2 \times 2)$ surface Brillouin zone (SBZ) of Si(001); the Kohn-Sham eigenstates are occupied according to a Fermi-Dirac distribution with $k_B T = 0.020 \text{ eV}$. Tests with a higher plane-wave cutoff, a denser \mathbf{k} -point sampling, and a larger vacuum region lead us to an estimate of 0.05 eV for the uncertainty in the relative adsorption energies on the clean and monohydride Si(001) surface. Relative adsorption energies on the DD row are converged to within approximately 0.10 eV.

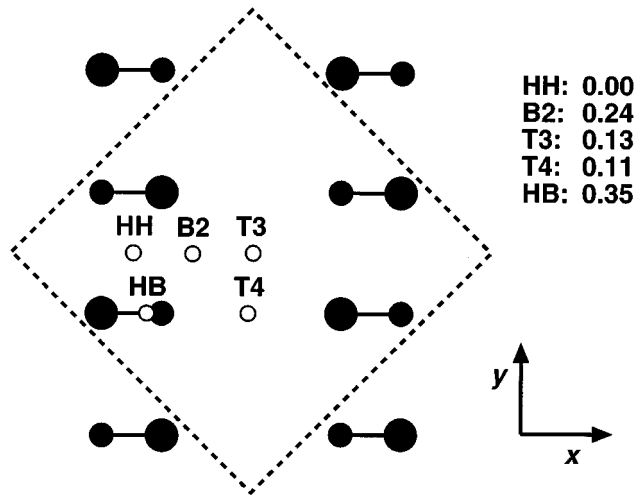


FIG. 1. Adsorption sites on the Si(001) surface. The black circles represent the Si atoms in the top layer of the surface, which are arranged in dimer rows (along the y direction); the smaller (larger) circles represent downwards (upwards) buckled atoms.¹⁶ The $c(4 \times 4)$ unit cell is indicated by the dashed line. The energies for adsorption of one Na atom are given relative to the HH site in eV.

Before considering Na adsorption on a DD row, we present results for Na adsorbed on the clean Si(001) surface and compare these to recent first-principles calculations of the Na covered Si(001) surface by Kobayashi *et al.*⁸ and Ko *et al.*¹⁵ In the present work a larger surface unit cell [$c(4 \times 4)$] is used to study adsorption in the low coverage regime. We expect that the relative adsorption energies of one Na atom in this unit cell are representative for single, isolated adsorbed atoms.⁷ The adsorption energies on the clean surface (and the corresponding electronic structure) will later be compared to those on the DD row. The clean Si(001) surface is characterized by rows of alternating buckled Si dimers in the top layer, shown schematically in Fig. 1. High-symmetry adsorption sites are labeled by their conventional names (see Ref. 8). The site labeled by HH is lowest in energy; the $T3$ and $T4$ sites represent local minima which are approximately 0.1 eV higher in energy. The $T3$ site is located in the middle between the dimer rows and the $T4$ site is slightly displaced (0.23 Å) towards the downwards buckled substrate atom. The HB site represents a saddle point on a path over a substrate dimer row (in the y direction). It was located by constraining the adatom to a plane perpendicular to the dimer rows and it is displaced by 0.34 Å with respect to the middle of the dimer row. For all the adsorption sites the substrate buckling remains unchanged upon sodium adsorption. Ko *et al.*¹⁵ found (for a higher sodium coverage) that an upward buckling of the substrate dimers towards the trough between two rows leads to a lower energy for the adsorption sites in this trough. We therefore recalculated the energies of the $T3$ and $T4$ configurations using this configuration for the substrate dimers. The energies of the $T3$ and $T4$ relative to the HH site become 0.05 eV and 0.16 eV, respectively, and are thus very similar to the ones given in Fig. 1. The small energy differences between the various adsorption sites indicate that adsorbed Na atoms are highly mobile at room temperature. The activation energy for diffusion in the trough between the dimer rows is negligible, i.e.,

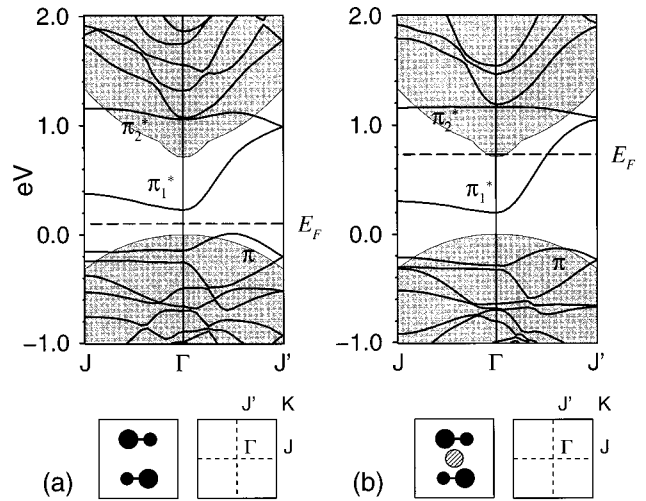


FIG. 2. Band structures of the (a) clean and (b) the Na covered ($1/4$ monolayer) Si(001)- $p(2 \times 2)$ surface along with the respective surface unit cells and Brillouin zones. The Fermi levels E_F are indicated by dashed lines, the shaded areas represent projections of the bulk bands. Energies are given with respect to the top of the bulk valence band.

within the error bar of the calculation. For diffusion along the HH - $T3$ path the activation energy is 0.25 eV. Similar high mobilities were also found for other metal atoms adsorbed on Si(001), such as aluminum.⁷

The calculated band structure of the clean Si(001) surface is shown in Fig. 2(a) in a $p(2 \times 2)$ surface cell; it is similar to that found in previous studies.¹⁶ The bonding combinations of the dangling bond surface states are labeled π , the antibonding combinations π_1^* and π_2^* . The π bands are filled and in the $\Gamma J'$ and ΓJ directions they are largely surface resonances, as shown in Fig. 2(a). The π_1^* band is empty and is a true surface band with a dispersion of 0.76 eV in the direction parallel to the dimer row ($\Gamma J'$). Perpendicular to the rows (ΓJ) its dispersion is 0.15 eV. The empty π_2^* band again is for the most part a surface resonance. In Fig. 2(b) the band structure is shown for a Si(001) surface on which one Na atom per $p(2 \times 2)$ cell is adsorbed at a HH site. It is very similar to the band structure of the clean surface. The major difference is that the π_1^* band is now half filled, which makes this Na covered surface metallic. The Na atoms have transferred their electrons to these π_1^* surface states. Similar results were obtained by Kobayashi *et al.*⁸ for the 2×1 Na covered Si(001) surface. In their case the Coulomb potential of the Na ions in addition results in a downward shift of the surface bands. For the low coverages which are used here, we find no evidence for such a shift. In the low coverage regime (at least up to $1/4$ of a monolayer) the shape and position of the surface bands with respect to the bulk states remain unaltered. The concentration of Na atoms only determines the position of the Fermi level within the fixed π_1^* band.

Na adsorption at a DD row is modeled in a $p(4 \times 2)$ unit cell, which contains two dimer rows, cf. Fig. 3(a). One of these rows is passivated by hydrogen atoms, which results in symmetric surface dimers. The other row represents the DD row and consists of $p(2 \times 2)$ buckled Si surface dimers as on the clean surface. The adsorption energies at the HH and

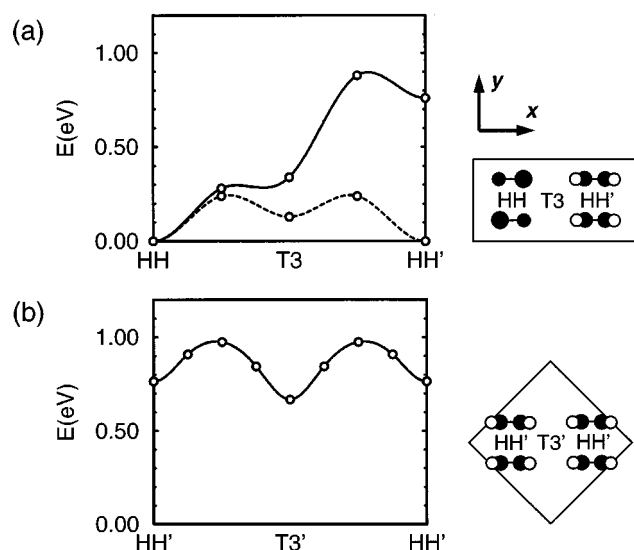


FIG. 3. (a) Relative energies for adsorption of a Na atom on a path along the x direction from the DD row to the hydrogen passivated dimer row, along with the unit cell used in the calculations. Notation as in Fig. 1; the open circles represent the hydrogen atoms. The dotted line denotes the corresponding energies for adsorption on the clean surface. (b) The corresponding energies (and the unit cell used) for adsorption on the monohydride Si(001) surface.

B2 sites on the DD row are equal within the error bar to the corresponding values at the clean Si(001) surface. We conclude that adsorption at a DD row is similar to adsorption at a dimer row on the clean Si(001) surface. Away from the DD row, towards the hydrogen passivated row, energies become much higher. This is shown in Fig. 3(a), where we plot relative energies for various adsorption sites on a straight line between the DD row and the hydrogen passivated row (in the x direction). Adsorption at the DD row is clearly favorable; the DD row traps adsorbing Na atoms. We have checked various other adsorption sites in between the DD and the passivated row. All of these have energies which are at least 0.3 eV higher than that of the HH site, so the latter is the most stable adsorption site. Based upon the results of Fig. 3(a), an estimate for the activation energy E_a for diffusion from the DD row onto the fully passivated surface is 0.9 eV. One can use this value to roughly estimate the jump rate Γ for this diffusion event, assuming a simple Arrhenius expression $\Gamma = A \exp(-E_a/k_B T)$. Using a typical value for the prefactor $A = 10^{13}$ Hz and $T = 300$ K, one finds $\Gamma = 0.007$ Hz, which would mean that diffusion from the DD row onto the passivated surface is a rare event and the Na atom is trapped at the DD row.¹⁷ In order that the DD row can actually capture Na atoms evaporated onto the surface, these atoms must of course be sufficiently mobile on the hydrogen passivated part of the surface. We have calculated energies along a path from the HH' to the $T3'$ site on the monohydride Si(001) surface, the results of which are shown in Fig. 3(b) (note that for this surface the $T3'$ site is lower in energy than the HH' site). The activation energy is 0.31 eV, which indicates that Na atoms are indeed quite mobile on the passivated surface (estimated jump rate 6×10^7 Hz). Having captured the Na atoms and confined them to the DD row, we estimate their mobility along this row. The diffusion path for sodium atoms parallel to the DD row (i.e., in the y direction)

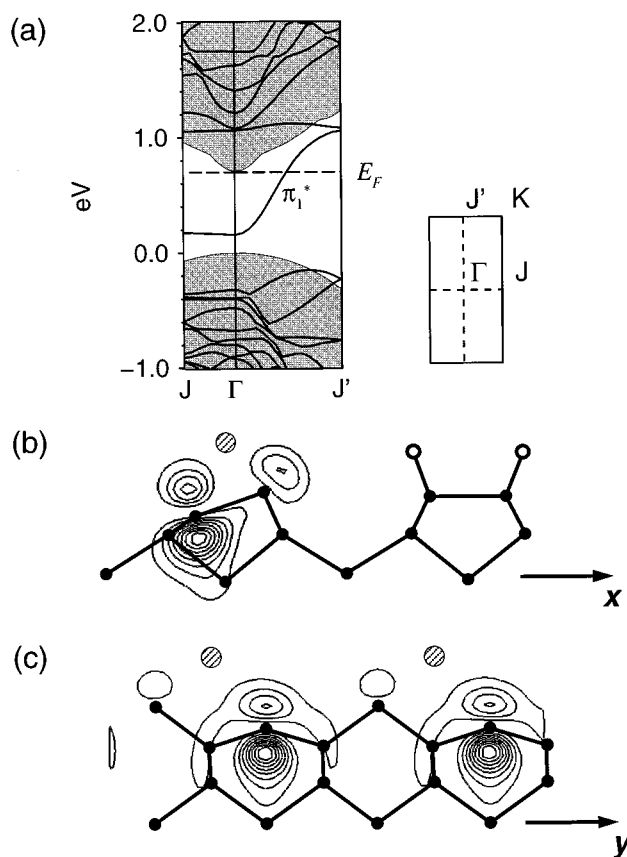


FIG. 4. (a) Band structure and surface Brillouin zone of the $p(4 \times 2)$ structure shown in Fig. 3(a) with one Na atom adsorbed at the HH site. (b) and (c) Plots of the electron density of the π_1^* state at Γ (b) in a vertical plane perpendicular to the dimer rows through one of the surface dimers, (c) in a vertical plane along the DD row passing through the downwards buckled dimer atoms. Si, H, and Na atoms are represented by filled, open, and hatched circles, respectively. The contour levels run from 1 to 8 in steps of 1 ($\times 10^{-3} a_0^{-3}$).

runs either on top of the DD row, or in between the DD and a neighboring passivated row. The activation energy of the first path is estimated to be 0.35 eV (cf. the energy of the saddle point HB , see Fig. 1). A lower bound for the activation energy of the second path is found by a minimization in which we constrain the sodium adatom to a plane perpendicular to the dimer rows, through the $T4$ site. This lower bound is 0.30 eV, which is our final estimate for the energy barrier for diffusion parallel to the DD row. It follows that the Na atoms are mobile along the DD row at room temperature; at temperatures below ~ 120 K their motion will be frozen (i.e., the jump rate will be much smaller than 1 Hz).

Having established the stability of a sodium-doped DD row, we now consider its electronic structure. The band structure of the $p(4 \times 2)$ unit cell with one Na atom adsorbed at the HH site, cf. Fig. 3(a), is shown in Fig. 4(a). The surface bands resemble those of the clean surface, cf. Fig. 2; they result from the dangling bonds of the Si atoms in the DD row. The π_1^* state of the DD row is half filled after Na adsorption and again the result is similar to Na adsorption on the clean surface [Fig. 2(b)]. Hydrogen passivation of the adjacent row leads to strong covalent bonds between the Si atoms of that row and the H atoms; the energies of the cor-

responding bonding states are well inside the Si bulk valence band. In addition the hydrogen passivated row reduces the dispersion of the DD surface bands in the direction perpendicular to the rows (ΓJ , Fig. 4). The dispersion along ΓJ is 0.02 eV [in the $p(4 \times 2)$ cell], as compared to 0.15 eV on the clean surface. So even when separated by only one hydrogen passivated row, as in the $p(4 \times 2)$ cell, the surface states of the DD row have a clear 1D character. This is illustrated by Figs. 4(b) and 4(c) which show plots of the π_1^* state at Γ . This state has antibonding character between the Si atoms of one depassivated dimer; it has p_z character on the downwards buckled Si atom and an sp^3 -like lobe on the upwards buckled atom (which reflects the sp^2 - and sp^3 -like hybridizations of the down- and upwards buckled dimer atoms, respectively). Clearly, this state is one dimensional.

Within the approximations used our calculations predict that the Na-doped DD row has metallic properties. We briefly speculate on additional effects which could open a gap and destroy the metallicity of this structure. If the on-site coulomb correlation energy becomes large as compared to the width of the surface band, the system could become a Mott-Hubbard insulator. The on-site correlation has been used in describing the electronic structure of the Na covered GaAs(110) surface.¹⁸ For the present system we expect this

effect to be much weaker, as the DD states are much more extended (see Fig. 4) than the GaAs(110) surface states. The electron-lattice interaction can also lead to the opening of a gap, which is especially likely in quasi-one-dimensional metallic systems where nesting of Fermi surfaces can trigger a Peierls distortion (but does not always have to, according to Littlewood and Heine¹⁹). The importance of this effect can be studied within the approximations used here. We have performed a geometry optimization using a $p(4 \times 4)$ unit cell with two Na atoms adsorbed at HH sites, i.e., the unit cell of Fig. 3(a) doubled in the direction of the dimer rows. We found no evidence for a spontaneous breaking of the translational symmetry and no corresponding opening of a gap at the Fermi level.

In conclusion we have shown that a depassivated dimer (DD) row on the monohydride Si(001) surface acts as an adsorption template for Na atoms. At room temperature the sodium atoms are sufficiently mobile to reach the DD row and subsequently become trapped at this row. The adatoms are still mobile along this row, but at a temperature below ~ 120 K their motion is completely frozen. The Na atoms transfer their electrons to the empty one-dimensional band of the DD row. A partial filling of this band leads to a one-dimensional metallic atomic wire.

-
- ¹See, e.g., G.D. Mahan, *Many-particle Physics* (Plenum, New York, 1990).
- ²M. F. Crommie, C. P. Lutz, and D. M. Eigler, *Science* **262**, 218 (1993).
- ³Q. J. Gu *et al.*, *Appl. Phys. Lett.* **66**, 1747 (1995).
- ⁴T.-C. Shen *et al.*, *Science* **268**, 1590 (1995).
- ⁵S. Watanabe *et al.*, *Phys. Rev. B* **52**, 10 768 (1995).
- ⁶T.-C. Shen, C. Wang, and J. R. Tucker, *Phys. Rev. Lett.* **78**, 1271 (1997).
- ⁷G. Brocks, P. J. Kelly, and R. Car, *Phys. Rev. Lett.* **70**, 2786 (1993); *J. Vac. Sci. Technol. B* **12**, 2705 (1994).
- ⁸K. Kobayashi *et al.*, *Phys. Rev. B* **45**, 3469 (1992).
- ⁹R. Car and M. Parrinello, *Phys. Rev. Lett.* **55**, 2471 (1985).
- ¹⁰L. Kleinman and D. M. Bylander, *Phys. Rev. Lett.* **48**, 1425 (1982).
- ¹¹G. B. Bachelet, D. R. Hamann, and M. Schlüter, *Phys. Rev. B* **26**, 4199 (1982).
- ¹²N. Troullier and J. L. Martins, *Phys. Rev. B* **43**, 1993 (1991).
- ¹³J. P. Perdew and A. Zunger, *Phys. Rev. B* **23**, 5048 (1981).
- ¹⁴S. G. Louie, S. Froyen, and M. L. Cohen, *Phys. Rev. B* **26**, 1738 (1982).
- ¹⁵Y.-J. Ko, K. J. Chang, and J.-Y. Yi, *Phys. Rev. B* **51**, 4329 (1995).
- ¹⁶A. Ramstad, G. Brocks, and P. J. Kelly, *Phys. Rev. B* **51**, 14 504 (1995), and references therein.
- ¹⁷Jump rates can only be given as order-of-magnitude estimates. Allowing for uncertainties in the activation energy or prefactor could, for instance, make the jump rate two orders of magnitude higher. Experimentally one has a finer control over the jump rate; instead of performing the experiment at room temperature, cooling down by ~ 40 K decreases the jump rate by two orders of magnitude.
- ¹⁸J. Hebenstreit and M. Scheffler, *Phys. Rev. B* **46**, 10 134 (1992); O. Pankratov and M. Scheffler, *Phys. Rev. Lett.* **70**, 351 (1993).
- ¹⁹P. B. Littlewood and V. Heine, *J. Phys. C* **14**, 2943 (1981).